International Conference on Artificial Reality and Telexistence
Eurographics Symposium on Virtual Environments (2022)
J.-M. Normand and H. Uchiyama (Editors)

Cast-Shadow Removal for Cooperative Adaptive Appearance Manipulation

Shoko Uesaka[1] and Toshiyuki Amano[†1]

[1]Graduate School of Systems Engineering, Wakayama University, Japan

Abstract

We propose a framework to suppress over-illumination at the overlapping area created by cooperative adaptive appearance manipulation with independently working two projector–camera systems. The proposed method estimates projection overlapping in each projector–camera unit with neither geometrical mapping nor projection image sharing. Then, the method suppresses the projection illumination of the overlapping area by compensated reflectance estimation. Experimental results using two projector–camera systems confirm that the proposed method correctly detects overlapping areas adaptively and removes cast shadows that cause uneven illumination owing to cooperative appearance manipulation of a moving 3D target.

CCS Concepts

• ***Human-centered computing*** → ***Mixed / augmented reality;*** • ***Computing methodologies*** → ***Mixed / augmented reality;***

1. Introduction

The shader lamps [RWLB01] enabled texture mapping on a 3D object. Since then, many applications and techniques have been proposed in the context of spatial augmented reality. In addition to displaying textures, 3D projection mapping can be used for optical restoration of damaged art objects [ALY08], reproduction of various reflectance properties [OOD10], representation of high-dynamic-range texture by contrast boosting on 3D printed objects [SIS11], augmentation of a physical avatar [BBG*13], and other applications. Moreover, 3D projection mapping has been studied for dynamic processes such as projection of textures drawn by user interactions on a freely movable rigid object with optical tracking [BRF01] and diminishable visual markers [AIS]. Similarly, dynamic projection mapping for complex-shaped objects using visual tracking with a virtual 3D model [RKK16], position sensing using a Kinect depth sensor [SCT*15], and projection pattern removal using an infrared camera [HKK17] have been proposed. Furthermore, dynamic projection mapping has been achieved for deformable objects based on visible dot clusters [NWI17] and invisible markers based on infrared ink [PIS14, FST*14].

Unlike projection mapping, spatial augmented reality is promising for appearance manipulation with a projector–camera system in a dynamic manner. Applications of appearance manipulation include vision support [AK10] and representation of embedded animation information on printed media using coded printing. In addition, appearance manipulation can induce illusory deformation. For instance, deformation lamps introduce illusory deformation [KFSN16], while swinging 3D lamps facilitate 3D optical illusions of motion parallax in 2D paintings [ONH17].

Employing a coaxial projector–camera optical setting facilitates successive appearance manipulation on a 3D object. This optical configuration and image processing algorithms from computer vision have been combined for materiality manipulation of the glossiness and transparency of opaque 3D objects [Ama13]. Additionally, multiple coaxial projector–camera units with mirror reflection enable appearance manipulation of the whole around a 3D object [ASUK14]. However, the units produce uneven projection illumination owing to the projection from separate projector–camera feedback that causes reflectance estimation errors in each projection unit.

We propose a method to solve projection illumination unevenness caused by cast shadow around a 3D object for appearance manipulation by estimating projection overlapping when using distributed coaxial multiple projector–camera systems.

2. Related work

2.1. 3D Apperanace Manipulation

The alignment of a coaxial projector and camera enables adaptive appearance manipulation on a 3D surface without rendering by using a 3D shape model and projection registration onto a 3D physical model, as shown in Figure 1. Appearance manipulation implemented on coaxial optics provides a fixed pixel mapping between the projection and captured images and enables interactive

† amano@wakayama-u.ac.jp

DOI: 10.2312/egve.20221271

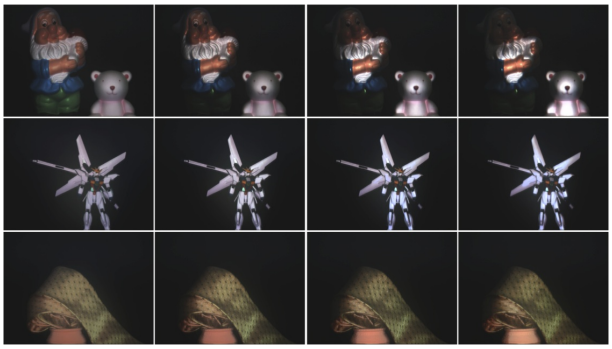

Figure 1: *Projection-based real-time material appearance manipulation [Ama13].*

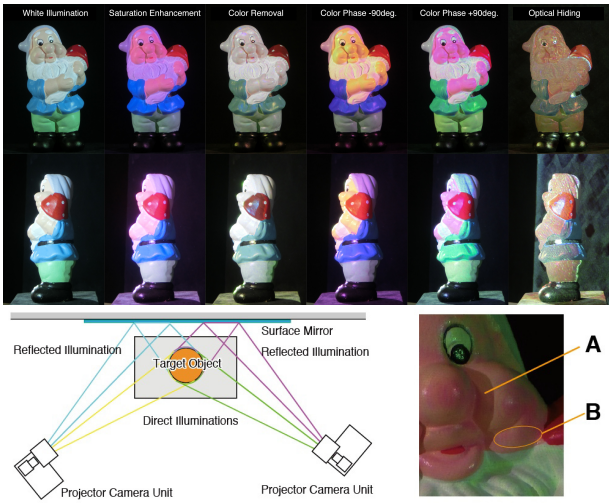

Figure 2: *Results of appearance manipulation around a circumference (top) and its optical setting (bottom left). Unevenness resembling cast shadow by projected illumination (bottom right) [ASUK14].*

projection based on 2D image processing. Appearance manipulation performs adaptive projection based on the reflectance of the target surface instead of mapping a prepared texture onto the target object. Its main difference with 3D projection mapping is its potential human vision support, visualization of hidden properties, and interactive appearance transformations of the materiality.

Although a coaxial projector–camera system enables adaptive appearance manipulation on a 3D surface, the manipulation area is limited by the projection. Therefore, it does not allow free viewing positions other than the projection region. This problem was overcome by appearance manipulation with multiple coaxial projector–camera units [ASUK14]. Such appearance manipulation around a circumference is achieved by projecting on backside reflection and using multiple units. However, as overlapping projection causes reflectance estimation errors in appearance manipulation, unevenness of projected illumination resembling cast shadows occurs, as shown in Figure 2. Considering overlapping projection from the geometric

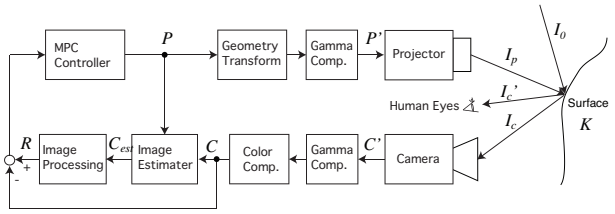

Figure 3: *Diagram of model predictive control (MPC) for appearance manipulation [AK10].*

relation between projection illuminations and the 3D shape of the projection target may solve this problem. However, this solution is inconvenient for appearance manipulation.

2.2. Shadow Removal for Cooperative Projection Mapping

Co-axial projector-camera configuration has been employed since the early work of radiometric compensation [FGN05]. This optical configuration ensures a fixed pixel mapping independent of the projection surface shape and enables dynamic adaptation. It potentially removes projection unevenness on the whole circumference of the 3D object by utilizing multiple projector-camera units. However, it is a radiometric compensation and requires a projection registration with tracking to achieve the projection mapping. Moreover, the radiometric compensation can not achieve appearance manipulation.

A shadow removal by the multiple distributed projector-camera feedback was proposed [TIK17]. This distributed system employed an error propagating scheme implementable in a distributed manner, enabling the prediction of the shadow region to achieve a radiometric compensation. Its scheme has the potential to predict the overlapping projection region and remove the cast shadow-like luminance unevenness. However, their method requires pixel correspondences among projection images. This means a target tracking and 3D shape model to obtain pixel corresponding for the entire circumference appearance manipulation, and thus it is not suitable for our purpose. We need to be found another mechanism of the luminance compensation that does not require any information sharing in the distribution manner.

3. Proposed Appearance Manipulation Method

Amano et al. [AK10] proposed appearance manipulation with projector–camera feedback using model predictive control as shown in Figure 3. The diagram shows the color intensity response between the projector, $\mathbf{P} \in \mathbb{R}^3$, and camera, $\mathbf{C} \in \mathbb{R}^3$, via the projection surface. During projection, the reflectance on the surface, $K \in \mathbb{R}^{3\times3}$, is estimated as

$$\hat{K} = diag\{\mathbf{C}./(M\mathbf{P}+\mathbf{C}_0)\} \quad (1)$$

where M is the color mixing matrix between the projector and camera, $\mathbf{C}_0$ is the environment illumination obtained by calibration, and $./$ denotes component-wise division. Based on $\hat{K}$, the true appearance that under the white light projection is given by

$$\mathbf{C}_{est} = \hat{K}\mathbf{C}_{white} \quad (2)$$

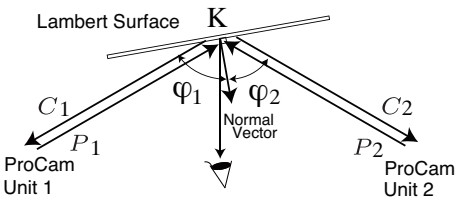

Figure 4: *Assumed scenario for cooperative projection.*

where $\mathbf{C}_{white} = (1,1,1)^T$. Then, the system generates control reference $\mathbf{R}$ by user-defined image processing and manipulates the object appearance by illumination projection using model predictive control. For saturation enhancement, control reference $\mathbf{R}$ is generated as

$$\mathbf{R} = gain\{(1+s)\mathbf{C}_{est} - s\mathbf{C}_m\}, \text{for } s > 0 \tag{3}$$

where $\mathbf{C}_m$ is monochromatic image of $\mathbf{C}_{est}(|\mathbf{C}_{est}|, |\mathbf{C}_{est}|, |\mathbf{C}_{est}|)$, s is a parameter that controls the saturation.When $s = 0$, there is no enhancement, and when $s > 0$, the saturation is enhanced. In addition, the brightness of control reference is changed by gain, and the apparent brightness can be controlled. For color phase shift, control reference $\mathbf{R}$ is generated as

$$\mathbf{R} = gain\mathbf{U}\mathbf{T}_r\mathbf{U}^T\mathbf{C}, \text{for } 0 < s < 1 \tag{4}$$

where $\mathbf{U}$ is RGB-Lab conversion and $\mathbf{T}_r$ is rotation matrix in a-b chroma plane.

3.1. Reflectance Estimation in Distributed System

When two projector–camera units cooperatively manipulate the appearance of a target object, control error occurs in the overlapping projection region. As both projections are irradiated from different angles, the apparent reflectance values obey the law of cosines, and we obtain the captured image as follows:

$$\mathbf{C}_i = \cos(\varphi_1)KM\mathbf{P}_1 + \cos(\varphi_2)KM\mathbf{P}_2 + \mathbf{C}_0 \tag{5}$$

where $i = 1,2$ is the unit number, φ_i is the incident angle of unit i, $\mathbf{P}_i$ is the projection from unit i, and K is the reflectance matrix measured with vertical incidence. We assume Lambert's surface reflection and that both units are placed at the same distance from the surface. Therefore, the same brightness is observed from both units. The main problem is the unknown projection from the other unit because the corresponding projection pixel is not known for the independently working distributed system.

In cooperative appearance manipulation, projections $\mathbf{P}_1$ and $\mathbf{P}_2$ converge to the same brightness for $\varphi_1 = \varphi_2$ [ASUK14]. In the scenario shown in Figure 4, the illumination contribution should be proportional to the incident angle by Lambert's cosine law. We define the following degree of contribution:

$$\eta_i = \frac{\cos(\varphi_i)}{\cos(\varphi_1) + \cos(\varphi_2)} \tag{6}$$

and estimate the projection from the other unit under this assumption. By using the degree of contribution, we obtain

$$\eta_1 KM\mathbf{P}_1 = \eta_2 KM\mathbf{P}_2. \tag{7}$$

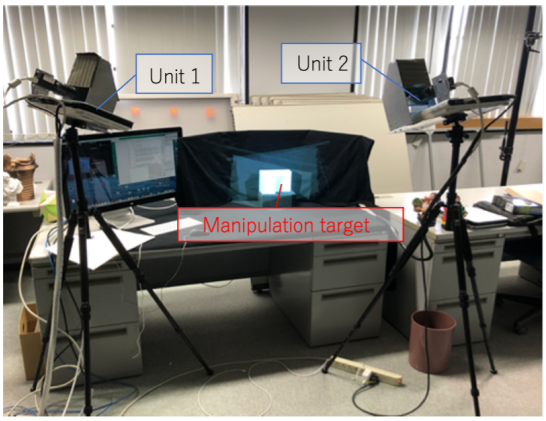

Figure 5: *Experimental setup.*

Then, $\mathbf{C}_1$ can be rewritten considering this constraint with equation (5) as

$$\mathbf{C}_i = \frac{\eta_1 + \eta_2}{\eta_i} K_i M\mathbf{P}_1 + \mathbf{C}_0 \tag{8}$$

where $K_i = \cos(\varphi_i)K$ is the apparent reflectance of unit i. Hence, we obtain the following compensated reflection estimation:

$$\hat{K}_i^* = \frac{\eta_i}{\eta_1 + \eta_2} diag\{\mathbf{C}_i./(M\mathbf{P}_i + \mathbf{C}_0)\} \tag{9}$$

that only requires the local information of each unit.

3.2. Adaptive Overlap Estimation

Eq. (9) describes the compensated reflectance under projection overlapping. To achieve cooperative appearance manipulation, we require successive state estimation to determine whether the projection illumination is overlapping. For this estimation, we determine the state from the estimated reflectance and obtain the reflectance matrix as follows:

1. Calculate reflectance $\hat{K}$ by Eq. (1) assuming nonoverlapping projection.
2. Estimate the overlap from average reflectance $trace(\hat{K})/3$ for a threshold determined experimentally.
3. Chose either $\hat{K}$ or $\hat{K}^*$ from the estimated overlapping state.

As the degree of contribution, η_i, changes by the incident angles depending on projector positions and surface normal, the surface shape and posture are required for accurate calculation. However, these requirements prevent adaptive processing. Instead, we measure η_i by preliminary calibration. First, we perform white planar projection between the units symmetrically. Then, we capture images $\mathbf{C}^{(1)}$ and $\mathbf{C}^{(2)}$ with white illumination projection from one projector, $\mathbf{C}^{(I+II)}$ with projection from both projectors, and $\mathbf{C}_0$ without projection. From these images, we obtain the degree of contribution per pixel for both units as follows:

$$\eta_i = \frac{|\mathbf{C}^{(i)}| - |\mathbf{C}_0|}{|\mathbf{C}^{(I+II)}| - |\mathbf{C}_0|}. \tag{10}$$

4. Experimental Results

Two coaxial projector–camera units were placed in front of a 3D target forming an angle of 120 degrees, as shown in Figure 5.We composed each unit with a USB 3.0 camera (XIMEA MC031CG-SY. 3.1 Mpix with cropping) and a 1280x800 resolution projector (CASIO XJ-A141). The experiment was conducted in an indoor lighting environment with a ceiling light. The irradiance on the target object was around 37 lx.As each unit worked independently in the distribution system, they performed adaptive appearance manipulation without sharing captured or projected images.

4.1. Over-illumination Suppression

We evaluated the illumination uniformity obtained from the proposed method and the method described in [ASUK14] on a 3D surface with a step edge. When both units projected white illumination, projection unevenness was caused by the cast shadow from the left projection, as shown in Figure 6. The second column shows the ground truth of the number of overlapping projections from each viewing position. The proposed method detected the overlapping, as shown in the third column. The figure shows the area where the projection by the two units is white and a single unit is black. The overlap is correctly estimated on the side surface of the target. However, our method incorrectly estimated the top surface owing to the small incident angle because such angle reduces the apparent reflectance below the predetermined threshold. This is a limitation of our adaptive overlap estimation.

We also evaluated the appearance manipulation results obtained from the proposed method using reflectance estimation compensation based on the estimation of the number of projections and the method described in [ASUK14], obtaining the results shown in Figure 7. Saturation enhancement was controlled by equation Eq. (3)($gain = 0.68, s = 0.6$). Color phase shift was controlled by equation Eq. (4)($gain = 0.47, s = -0.6$).

The results show that the proposed method reduces the projection illumination unevenness by suppressing illumination in the overlapping area. Figure 8 shows the illumination profiles of appearance manipulation along segment A-A' in Figure 7 for both methods. The yellow arrows show regions manipulated with two units (overlapping), and the black arrow shows the region manipulated with a single unit (non-overlapping). To evaluate the manipulation accuracy, we examined the error of the overlapping area relative to the non-overlapping area.The comparison method has an average error of 17%, which is reduced to 4% by using the proposed method.

The effectiveness of our proposal was further confirmed in projection images, as those shown in Figure 9. As the comparison method cannot detect overlapping projections, the entire area of the manipulation target was uniformly illuminated. In contrast, the proposed method with independently working projector–camera units suppressed the projection intensity at the overlapping area and removed illumination unevenness resembling cast shadows.

4.2. Successive manipulation for the moving target

To evaluate the performance of excess projection suppression, we compared projections in dynamic scenes for the comparison and proposed methods. We applied color phase shift for appearance manipulation in both units. Then, we placed a dwarf figure as the manipulation target between both units and continuously moved it manually, as shown in Figure 10, where each row shows snapshots at a timestep. The shadow cast by the nose when using the comparison method was correctly manipulated because no disturbance

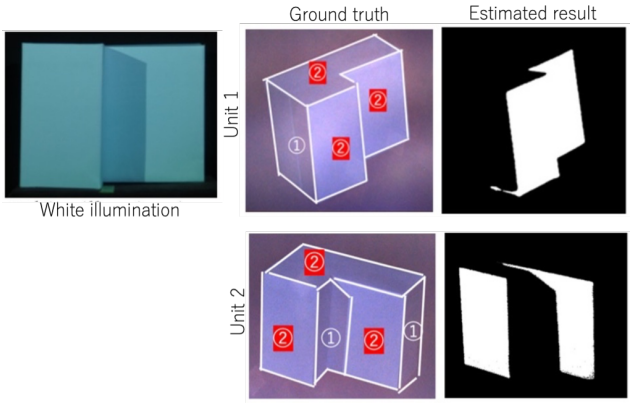

Figure 6: *Manipulation target and overlapping estimation results.*

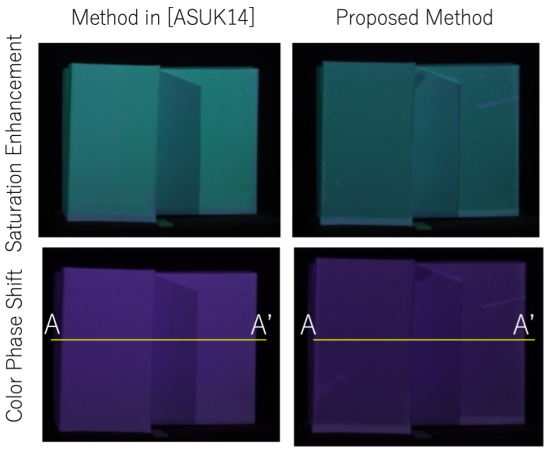

Figure 7: *Illumination unevenness from comparison and proposed methods.*

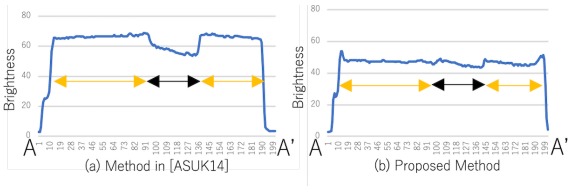

Figure 8: *Brightness variation along segment AA' for comparison and proposed methods.*

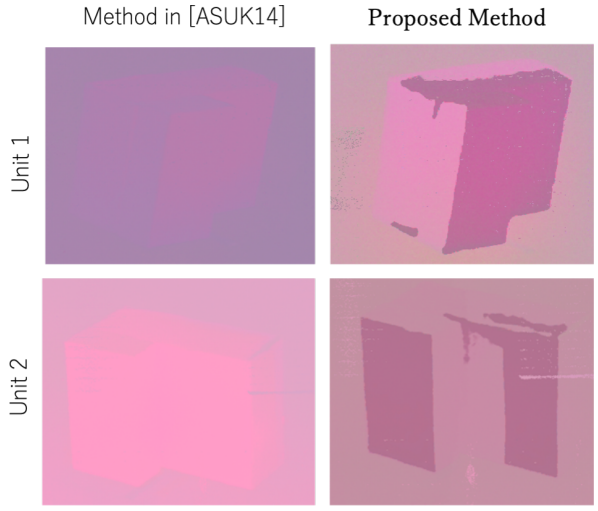

Figure 9: *Successive Appearance Manipulation on Moving Target*

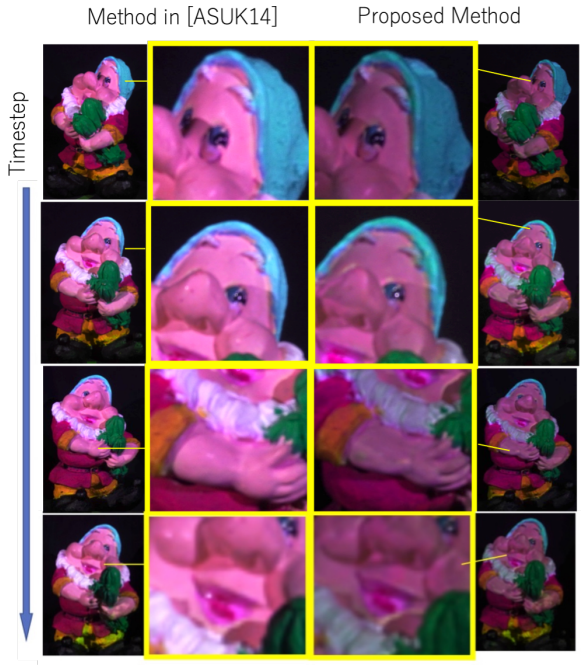

Figure 10: *Step-by-step comparison of projections in dynamic scenes.*

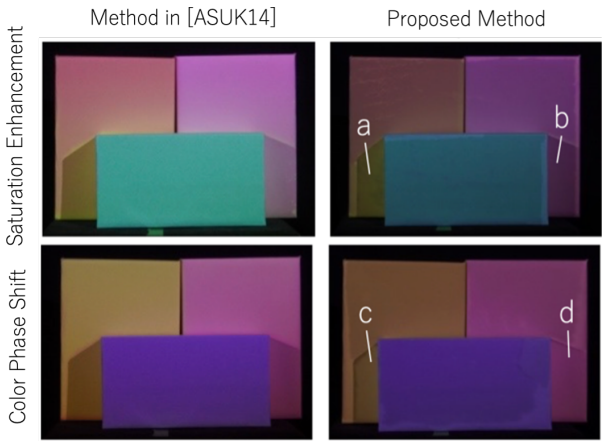

Figure 11: *Projection errors according to projection color.*

5. Discussions

We evaluated the appearance manipulation quality of the proposed and comparison methods on various surface colors, obtaining the results shown in Figure 11. The proposed method reduced projection illumination unevenness by cast shadows for most colored surfaces. However, when comparing areas a and b or c and d, the compensation error differed according to the color of the reflective surface. In addition, even for the same surface color, comparing a and b or c and d, the error differed depending on the type of operation, possibly owing to the different characteristics of the projectors. When the color mixing matrices of units 1 and 2 are M_1 and M_2, respectively, and the columns corresponding to each channel of these reflection matrices are $\mathbf{m}_i^R$, $\mathbf{m}_i^G$, and $\mathbf{m}_i^B$, the degree of contribution of the red, green, and blue projections are respectively given by

$$\eta_i^R = \frac{\cos(\varphi_i)|K\mathbf{m}_i^R|}{\cos(\varphi_1)|K\mathbf{m}_1^R| + \cos(\varphi_2)|K\mathbf{m}_2^R|}, \tag{11}$$

$$\eta_i^G = \frac{\cos(\varphi_i)|K\mathbf{m}_i^G|}{\cos(\varphi_1)|K\mathbf{m}_1^G| + \cos(\varphi_2)|K\mathbf{m}_2^G|}, \tag{12}$$

$$\eta_i^B = \frac{\cos(\varphi_i)|K\mathbf{m}_i^B|}{\cos(\varphi_1)|K\mathbf{m}_1^B| + \cos(\varphi_2)|K\mathbf{m}_2^B|}. \tag{13}$$

from the other unit appeared. However, excess projections appeared in other areas and required suppression to equalize brightness. In contrast, the proposed method suppressed excess projections and shadows cast on the face by adaptive processing. The remnants of excess illumination at the boundaries of the cast shadow persisted owing to the misalignment of adaptive overlap estimation. Thus, the accuracy and resolution of our method should be further improved in future work.

Hence, we can confirm that the degree of contributions is equivalent to equation (10) for $M_1 = M_2$. However, the degree of contribution changes according to the color of the projection owing to the projector characteristics and color K of the target.This does not occur if the characteristics are perfectly identical. However, although we employed the same products, individual differences exist, leading to this uneven illumination.In future research, we will investigate the compensation of projection considering color.

6. Conclusions

We propose a framework for dynamic projection illumination compensation on overlapping projection areas for cooperative adaptive appearance manipulation using two projector–camera systems. Experimental results confirm the effectiveness of the proposed method for correctly detecting overlapping areas adaptively and removing illumination unevenness resembling cast shadows created by cooperative appearance manipulation of a moving 3D target. However, as the degree of contribution of the projections changes according to the surface color, the illumination unevenness indicates divergence from the calibrated value. In addition, excess illumination occurs on the boundary of the overlapping area owing to misalignment in the adaptive overlap estimation. We will address these problems in future work.

References

[AIS] ASAYAMA H., IWAI D., SATO K.: Diminishable visual markers on fabricated projection object for dynamic spatial augmented reality, year = 2015. *SIGGRAPH Asia 2015 Emerging Technologies on - SA '15*, 1–2. doi:10.1145/2818466.2818477. 1

[AK10] AMANO T., KATO H.: Appearance control by projector camera feedback for visually impaired. pp. 57 – 63. doi:10.1109/CVPRW.2010.5543478. 1, 2

[ALY08] ALIAGA D. G., LAW A. J., YEUNG Y. H.: A virtual restoration stage for real-world objects. *ACM Trans. Graph. 27*, 5 (Dec. 2008), 149:1–149:10. URL: http://doi.acm.org/10.1145/1409060.1409102, doi:10.1145/1409060.1409102. 1

[Ama13] AMANO T.: Projection based real-time material appearance manipulation. In *Computer Vision and Pattern Recognition Workshops (CVPRW), 2013 IEEE Conference on* (June 2013), pp. 918–923. doi:10.1109/CVPRW.2013.135. 1, 2

[ASUK14] AMANO T., SHIMANA I., USHIDA S., KONO K.: Successive Wide Viewing Angle Appearance Manipulation with Dual Projector Camera Systems. In *Proceedings of the 24th International Conference on Artificial Reality and Telexistence and the 19th Eurographics Symposium on Virtual Environments* (Aire-la-Ville, Switzerland, Switzerland, 2014), ICAT - EGVE '14, Eurographics Association, pp. 49–54. doi:10.2312/ve.20141364. 1, 2, 3, 4

[BBG*13] BERMANO A., BRÜSCHWEILER P., GRUNDHOFER A., IWAI D., BICKEL B., GROSS M.: Augmenting physical avatars using projector-based illumination. *ACM Transactions on Graphics 32*, 6 (2013), 189:1–10. URL: http://dl.acm.org/citation.cfm?id=2508416, doi:10.1145/2508363.2508416. 1

[BRF01] BANDYOPADHYAY D., RASKAR R., FUCHS H.: Dynamic shader lamps : painting on movable objects. In *Proceedings IEEE and ACM International Symposium on Augmented Reality* (2001), pp. 207–216. doi:10.1109/ISAR.2001.970539. 1

[FGN05] FUJII K., GROSSBERG M., NAYAR S.: A projector-camera system with real-time photometric adaptation for dynamic environments. *2005 IEEE Computer Society Conference on Computer Vision and Pattern Recognition (CVPR'05)* (2005), 814–821 vol. 1. URL: http://ieeexplore.ieee.org/lpdocs/epic03/wrapper.htm?arnumber=1467351, doi:10.1109/CVPR.2005.41. 2

[FST*14] FUJIMOTO Y., SMITH R. T., TAKETOMI T., YAMAMOTO G., MIYAZAKI J., KATO H.: Geometrically-Correct Projection-Based Texture Mapping onto a Deformable Object. 169–170. doi:10.1109/VR.2014.6802105. 1

[HKK17] HASHIMOTO N., KOIZUMI R., KOBAYASHI D.: Dynamic projection mapping with a single ir camera. *International Journal of Computer Games Technology 2017* (2017), 4936285. URL: https://doi.org/10.1155/2017/4936285, doi:10.1155/2017/4936285. 1

[KFSN16] KAWABE T., FUKIAGE T., SAWAYAMA M., NISHIDA S.: Deformation Lamps. *ACM Transactions on Applied Perception 13*, 2 (2016), 1–17. URL: http://dl.acm.org/citation.cfm?doid=2888406.2874358, arXiv:1509.08037, doi:10.1145/2874358. 1

[NWI17] NARITA G., WATANABE Y., ISHIKAWA M.: Dynamic projection mapping onto deforming non-rigid surface using deformable dot cluster marker. *IEEE Transactions on Visualization and Computer Graphics 23*, 3 (Mar. 2017), 1235–1248. URL: https://doi.org/10.1109/TVCG.2016.2592910, doi:10.1109/TVCG.2016.2592910. 1

[ONH17] OGAWA N., NARUMI T., HIROSE M.: Swinging 3D lamps. *ACM SIGGRAPH 2017 Posters on - SIGGRAPH '17* (2017), 1–2. URL: http://dl.acm.org/citation.cfm?doid=3102163.3102230, doi:10.1145/3102163.3102230. 1

[OOD10] OKAZAKI T., OKATANI T., DEGUCHI K.: A Projector-Camera System for High-Quality Synthesis of Virtual Reflectance on Real Object Surfaces. *IPSJ Transactions on Computer Vision and Applications 2* (2010), 71–83. doi:10.2197/ipsjtcva.2.71. 1

[PIS14] PUNPONGSANON P., IWAI D., SATO K.: Projection-based visualization of tangential deformation of nonrigid surface by deformation estimation using infrared texture. *Virtual Reality 19* (12 2014), 45–56. doi:10.1007/s10055-014-0256-y. 1

[RKK16] RESCH C., KEITLER P., KLINKER G.: Sticky projections-a model-based approach to interactive shader lamps tracking. *IEEE Transactions on Visualization and Computer Graphics 22*, 3 (2016), 1291–1301. doi:10.1109/TVCG.2015.2450934. 1

[RWLB01] RASKAR R., WELCH G., LOW K.-L., BANDYOPADHYAY D.: Shader lamps: Animating real objects with image-based illumination. In *Proc. of the 12th Eurographics Workshop on Rendering Techniques* (2001), pp. 89–102. 1

[SCT*15] SIEGL C., COLAIANNI M., THIES L., THIES J., ZOLLHÖFER M., IZADI S., STAMMINGER M., BAUER F.: Real-time pixel luminance optimization for dynamic multi-projection mapping. *ACM Trans. Graph. 34*, 6 (Oct. 2015). URL: https://doi.org/10.1145/2816795.2818111, doi:10.1145/2816795.2818111. 1

[SIS11] SHIMAZU S., IWAI D., SATO K.: 3d high dynamic range display system. In *Proceedings of the 2011 10th IEEE International Symposium on Mixed and Augmented Reality* (2011), ISMAR '11, pp. 235–236. URL: http://dx.doi.org/10.1109/ISMAR.2011.6092393, doi:10.1109/ISMAR.2011.6092393. 1

[TIK17] TSUKAMOTO J., IWAI D., KASHIMA K.: Distributed Optimization Framework for Shadow Removal in Multi-Projection Systems. *Computer Graphics Forum 36*, 8 (2017), 369–379. doi:10.1111/cgf.13085. 2